A MICROGRAVITY VIBRATION ISOLATION RIG

Bibhuti B. Banerjee
Carl R. Knospe
Paul E. Allaire

Center for Magnetic Bearings/ROMAC
University of Virginia
Charlottesville, VA 22903 USA

1. ABSTRACT

It is well–known that the spacecraft environment deviates from a state of zero gravity due to various random as well as repetitive sources. Science experiments that require a microgravity environment must therefore be isolated from these disturbances. Active control of noncontact magnetic actuators enables such isolation. A one–degree–of–freedom test rig has been constructed to demonstrate the isolation capability achievable using magnetic actuators. A cylindrical mass on noncontacting electromagnetic supports simulates a microgravity experiment on board an orbiter. Disturbances generated by an electrodynamic shaker are transmitted to the mass via air dashpots representing umbilicals. A compact Lorentz actuator has been designed to provide attenuation of this disturbance.

2. INTRODUCTION

Space exploration was initiated for the investigation of space itself, ranging from the planetary system to the limits of the universe. Resulting benefits of this effort include satellite communications and earth observation and imaging systems. The scope of space exploration widened in the early eighties with the development of the space shuttle – a system capable of transporting a large cargo to a low earth orbit, and recovering the payload or frequently servicing it in space. A parallel development was the gradual change in the role of man in space, starting with the primarily technical function of a pilot and evolving into a more active involvement encompassing interactive work and scientific experimentation in space. Space–based laboratories like the Skylab and the Spacelab were flown to utilize the "vanishingly low" gravitational forces available for extended periods of time. The results, however, were mixed at best, and disappointing in certain cases. This can be explained in part by the fact that the environment aboard the spacecrafts deviates considerably from the ideal of zero gravity due to disturbances produced by machinery and people on board, thruster fire, and other factors.

The incentives for performing science experiments in space include the investigation of phenomena that are influenced by gravity on earth, the development of novel materials and the improvement of processes like crystal

---

This work was supported in part by the NASA Lewis Research Center and the Center for Innovative Technology of the Commonwealth of Virginia.

growth [1]. In theory, a freely orbiting spacecraft offers a state of zero gravity to objects inside it, since the gravitational force is balanced by the centrifugal force [2]. However, in practice, there are various residual forces that disturb the environment.

Attempts to estimate these residual forces have been made in the past few years [3–10]. The orbital microgravity environment can be divided into three classes, as detailed in Table 1. Quasi–steady accelerations are generated by three sources — gravity gradient, aerodynamic drag and rotational acceleration. Any point of an orbiting structure that is at a distance from the structure's center of mass experiences a gravitational field that is different from that at the spacecraft center of mass. Aerodynamic drag due to the earth's atmosphere represents the absolute lower limit of the achievable background microgravity level, if the effect of light pressure is neglected. Finally, in order to keep the same vertical orientation on the space station with respect to the earth, the station must maintain a constant pitch rate about its center of mass. This creates a centripetal force that results in a rotational acceleration.

Orbital thruster fire and the steady–state operation of machinery like fans and pumps on board a spacecraft are among the sources of periodic accelerations, which occur at known frequencies. Impulsive disturbances like crew push–off and the start–up and shut–down of machinery create non–periodic accelerations. The irregular, unpredictable nature of these accelerations complicates attempts at isolation.

Theoretical acceleration requirements for various processes and experimental conditions have been investigated [3,7,11]. The common feature of curves depicting the frequency–dependent requirements is that, for a given process, the acceleration threshold is lowest from steady–state to about (0.01 — 0.1) Hz, depending upon the type of experiment. The acceptable acceleration then increases linearly with increasing frequency, up to (1 — 10) Hz. Subsequently, it increases as the square of the frequency. The acceleration tolerance also typically scales inversely with the volume that characterizes the process. The slopes and breakpoints result from fundamental aspects of a process, and the shape of the curve can be considered to be characteristic of a family of experiments. The acceleration level thresholds range from an extreme level of $(10^{-7} - 10^{-8})$ g_0 for some material science and fluid science experiments, to only 10^{-3} g_0 for the majority of biology and biotechnology experiments.

A comparison of the microgravity requirements with the actual environment available on the spacecraft indicates the need for vibration isolation. Moreover, the frequency range of interest spans several decades, thus requiring the use of multiple strategies for isolation.

For the high frequency range, passive isolators can serve adequately. Since these are relatively simple and cheap, they can be placed at each interface between a disturbance source and the space station. It should be noted that the sensitivity of various categories of experiments to high frequency disturbances is also comparatively low.

In the quasi–static frequency range, the extremely low stiffness and large motion required make attempts at isolation very difficult. Rattlespace constraints prohibit the occurrence of such large relative motions between the payload and the spacecraft. This imposes a fundamental limitation upon vibration isolation. Consequently, efforts at minimizing the input disturbances, like reducing the surface area presented to the atmosphere so as to reduce atmospheric drag and locating

payloads as close to the spacecraft's center of mass as possible, are necessary. Owens and Jones have also suggested the possibility of canceling such disturbances by continuous thruster control of the whole spacecraft [11].

At intermediate frequencies — approximately between 0.01 Hz and 1 Hz — no passive isolation scheme can be effective due to the displacements and isolation levels required. Only active vibration isolation at the payload–spacecraft interface allows the synthesis of the desired isolator properties and the adjustment of these properties using a control loop.

The actuator used to implement an active control scheme in the intermediate frequency range should ideally be noncontacting. The ideas of acoustic, electrostatic and electromagnetic (Lorentz force) levitation have been considered in the context of containerless processing of materials in a low gravity environment [12–15]. The first two techniques are limited to small objects. Lorentz forces are utilized by placing an electrically conductive sample within a suitably designed coil excited by a radio frequency current. Currents induced in the sample interact with the magnetic field of the coil to produce forces that tend to move the sample away from regions of high magnetic flux density. These currents also tend to heat the sample, which is often utilized to melt it. However, the inability to control this heating effect independently of the coil current required for levitation is a limitation of this technique. Some unwanted stirring of a melt by the induced currents also occurs.

Noncontact magnetic actuators, utilizing electromagnets or permanent magnets, appear to be the best solution for vibration isolation in the intermediate frequency range [16]. These actuators produce relatively large forces and can be applied to the isolation of a variety of science experiments. An active magnetic isolation system can be "tuned" by simply changing control law gains to accommodate changes in the payload or the expected disturbance environment, or to produce improved performance once in orbit. Such experiments need only be enclosed in a container, and can have umbilicals connecting them to the spacecraft.

A Long Action Magnetic Actuator (LAMA) has been proposed for this purpose [17]. This is a magnetic thrust bearing modified to accommodate longer strokes than those found in typical industrial applications. The pole–faces are inclined at an acute angle to the axis of motion, instead of being perpendicular to it. Detailed studies of magnetic thrust bearing design and use have been made [18–20]. The LAMA would be suitable for those intermediate frequencies that require motions not exceeding about a hundred miles. Since the forces called for are of the order of a few pounds at most, such actuators can be quite compact, the size being primarily determined by the stroke required.

A single–axis magnetic actuator similar to a magnetic thrust bearing has been described in [21]. The authors compared various sensing options to close the actuator control loop — gap and current sensing, force sensing and flux sensing. In their experiment, the authors achieved force linearization using flux feedback. Due to shaker and accelerometer limitations, the lowest recorded frequency of their measured data was 5 Hz. A subsequent paper described a similar isolation system extended to six degrees–of–freedom, called the Fluids Experiment Apparatus Magnetic Isolation System (FEAMIS) [22].

An interesting dual–mode approach to vibration isolation of large payloads over long displacements has been discussed in [23]. It was intended to provide the high performance active isolation of noncontact magnetic suspension technology without the limitations on articulation imposed by the small air gaps used in such

systems. In such a tandem system, a "coarse" motion actuator was controlled as a followup actuator, always attempting to keep the gap displacement for the magnetic actuator within its design limits. The magnetic actuator functioned as a "fine" motion actuator, ignoring the presence of the other, coarse actuator. The performance requirements on the coarse actuator were not very stringent, since the imperfections of its motions would be attenuated by the fine actuator.

The operation of microgravity science experiments is likely to require the use of an umbilical. An example is a plastic tube formed into a helical shape and carrying a coolant. Acceleration control to reject disturbances caused by the compliance of the umbilical has been theoretically investigated [24]. The umbilical was assumed to have stiffness, but not damping. The microgravity quality deteriorated with increasing umbilical stiffness, as expected. Acceleration control improved disturbance rejection greatly when compared to position–only control, but there was a price to be paid in the form of a more complicated control system. An active umbilical control strategy, in which the extension of the umbilical is minimized by making one end track the other, was also analyzed. It was found to be effective in principle and comparable in performance to the acceleration control loop technique.

3. EXPERIMENTAL RIG

An experimental rig to demonstrate vibration isolation down to microgravity levels in one degree–of–freedom has been constructed, and is shown in Figures 1 and 2. An innovative long stroke Lorentz actuator, described in detail in the next section, will be used to implement the isolation scheme.

An electrodynamic shaker with a long, peak–to–peak stroke of 6.25 inches represents the space platform. The shaker is mounted, via aluminum plates, on a concrete block resting on the laboratory floor. The shaker can generate sinusoidal, random or impulse waveforms at frequencies down to DC, thus simulating the disturbances typically produced on a space station that require active isolation.

The umbilicals connecting a science experiment to the space platform are expected to be flexible hoses and wires. These will be modeled by air dashpots with adjustable stiffness and damping coefficients. This type of dashpot has been evaluated at NASA Lewis in a single–degree–of–freedom mass–spring–damper system in a fixed–fixed mounting configuration [25]. The test indicated the possibility of a nonlinear stiffness/damping mechanism in these air dashpots. The vibration isolation rig has been designed so that different kinds of umbilicals may be employed, including actual hoses used for fluid transfer. This is important, since very little work has been done to date on vibration isolation to microgravity levels in the presence of an actual physical connection between the experiment and the space platform.

The long stroke Lorentz actuator, in parallel to the umbilical(s), connects the shaker armature to the mass representing a microgravity science experiment in space. This mass is a solid steel cylinder weighing 75 pounds, which is a typical weight for such an experiment. The cylinder is horizontally suspended in space by the magnetic forces generated by a noncontact electromagnetic support system. Similar to radial magnetic bearings, the support system consists of two eight–pole structures, mounted on a concrete base, at the two ends of the cylindrical mass. This concrete base is massive compared to the "experiment" mass, and rests on the same laboratory floor as the separate concrete block on which the shaker is

mounted. Eddy current probes sense the radial position of the cylinder and complete the feedback loop supplying current to the electromagnets. When the electromagnetic support system is turned off, the cylinder rests on a pair of touchdown pedestals made of delrin.

The axial acceleration of the cylinder will be sensed off a sensory plate mounted at its free end, using a very low frequency accelerometer with a maximum resolution of 1 μg. Provision has been made for the use of other types of accelerometers, and the sensing of other states of the system, like position. The accelerometer signal will be fed to a feedback control circuit that determines the current required in the electromagnetic actuator to isolate the cylinder from the disturbances generated by the shaker. A control strategy for such an isolation system with multiple degrees–of–freedom is discussed in [26].

The background vibration levels on the concrete base on which the cylinder is mounted have been measured over twenty–four–hour periods, in both the horizontal and the vertical directions. These vibrations are of the order of milli–g's, the quietest period occurring from late in the night to early in the morning. Operating at this time will yield the highest degree of reproducibility in our results. Figures 3 and 4 show the frequency spectrum of the background acceleration in the horizontal and vertical directions. The vertical vibration shows acceleration components corresponding to natural frequencies of the mounting plate. The horizontal vibration has significant content at 45 Hz. The authors believe this is a floor mode.

4. THE LONG–STROKE LORENTZ ACTUATOR

A compact long–stroke Lorentz Actuator has been designed, built and tested in the laboratory. An intermediate version of the design was presented at the Workshop on Aerospace Applications of Magnetic Suspension Technology at NASA Langley in September, 1990 [27]. The final design described here incorporates many of the same features, but is much more linear with coil position. This was accomplished through modification of the flux distribution.

A schematic of the typical Lorentz Actuator, along with the terminology used, is shown in Figure 5. The current carrying coil moves in and out along the core. A strong permanent magnet in the shell maintains a constant magnetic flux in the cylindrical air gap across the pole faces, irrespective of the current in the coil (within design limits). The Lorentz force generated, therefore, can be linearly varied with coil current [28].

The requirements for the laboratory prototype were fixed at a total stroke of two inches and enough force capability to isolate a mass of 75 lbs. connected by an umbilical (air dashpot) to a source generating very low frequency vibrations. Force linearity with position and with current were also required. Moreover, in view of the ultimate goal of deployment in space, such a device had to be compact and lightweight. Low power consumption and low heat generation during operation were also important.

A computer program was written to implement a simple design algorithm for a Lorentz Actuator. The steps of this algorithm are presented in Figure 6.

Using a permanent magnet material with a very high maximum energy product of 35 MGOe (mega–Gauss–Oersted) [29] resulted in a design that required

a ring magnet of 3.20 in. outer diameter. The magnet manufacturer, however, could make such a magnet in one piece only if its outer diameter were less than 2 in.; making a ring magnet with a 3.20 in. outer diameter would have required the costly assembly of multiple segments, with an escalation of costs.

The possibility of designing a Lorentz Actuator satisfying all the requirements, with the outer diameter of the magnet being additionally constrained to less than 2 in., was therefore explored. The significant parameter in this context is the gap ratio, defined as the ratio of the shell–to–core air gap to the pole–face–to–core air gap. Conventional designs use ratios of 5:1 or higher in order to minimize leakage of magnetic flux from the shell to the core. Figures produced by the design program suggested that the design requirements could be met, along with the additional constraint, if the rule of thumb of using a gap ratio of 5:1 or more were drastically violated. Apparently, flux leakage, which the computer program did not take into account, would result in the failure of such a design. It was then hypothesized that this would not necessarily be the case if the core of the actuator were saturated during normal operation. The permeability of a saturated ferromagnetic material approaches that of air, and so most of the leakage that would have occurred, with such a low gap ratio (less than 2:1) and an unsaturated core, would be prevented.

A good way of verifying this hypothesis, without actually building such an actuator, is the use of finite element analysis. A commercially available magnetic finite element analysis package, MAGGIE, with a nonlinear modeling capability, was chosen. It also allowed us to take leakage and fringing into account, and different materials and geometries could be "tested" with relative ease.

A number of designs incorporating various features, were analyzed using the finite element analysis package. The finite element model was generated so as to achieve as much accuracy as possible, within hardware limitations. The mesh consists predominantly of quad elements. Infinite air elements, used earlier, were found to cause severe restrictions on mesh fineness. A mesh with only about 100 elements could be used. An air thickness of an inch on three sides of the axisymmetric model was specified instead. This was determined to be as accurate as having infinite air elements on all three sides for a model of this size, while a relatively fine mesh with about 400 elements could be used without encountering core memory limitations. Moreover, the finest mesh allowed by the configuration of our 386–based personal computer was used for the analysis.

Position linearity was improved, relative to the intermediate design, by increasing the length of the magnet, imparting a lip to it by reducing the shell outer diameter, and reducing the core diameter. The gap ratio resulting from the last change mentioned above is still only 1.47:1 – much smaller than a typically specified value of 5:1. The use of such an unconventionally low gap ratio enabled the design of a compact and lightweight actuator. Use of a large ratio would also have required a large diameter magnet that could not be made in one piece, thus increasing costs. The decrease in flux, and therefore force, caused by the increase in the length of the magnet was compensated, to some extent, by a reduction in the inner diameter of the magnet and a doubling of the pole piece thickness. Figure 7 shows the design. The overall length of the actuator is 4 in., while the outer diameter is only 1.95 in..

The salient features of the final design of the compact Lorentz Actuator are described below:

• Long Stroke — The requirement of two inches of total stroke is satisfied.

• Position Linearity — Over the whole two inches of stroke, the actuator exhibits a high degree of linearity. For a constant coil current, this means that the actuator force is the same irrespective of the axial position of the coil, within the stroke bounds. Figures 8 and 9 depict this relationship for positive and negative coil currents respectively. Note that flux leakage has been reduced to almost zero over the shell–to–core gap to achieve this. The maximum flux density across the shell–to–core gap is only about 7% of the maximum flux density across the pole–face gap.

• Current Linearity — This requires that the average flux density in the effective air gap remain constant with variations in the coil current between the upper and the lower limits. This is indeed the case, resulting in force vs. current linearity, Figure 10.

• Force — A maximum force of 1.25 lbs is produced by this actuator, which is sufficient for our needs. This peak force requires a coil current of 2.5 A.

• Weight — At 2.28 lb., this actuator is only a tenth of a pound heavier than the previous design.

• Current Density — A value of 1000 A/sq. in. in continuous use ensures cool operation. For peak loads, a fivefold increase in current density is possible.

• Materials — The magnet is made of neodymium iron boron, which has a very high maximum energy density product of 35 MGOe. Selection of such a material helped make the design compact. The high permeability circuit material is a 48% nickel–iron alloy that saturates at 15 kG. The B–H curve for this material, provided by the manufacturer, was input to MAGGIE as a table of a large number of points on the curve. This was necessary because a nonlinear material characteristic was being modeled.

The design specifications of the Lorentz Actuator are detailed in Table 2. This actuator was built and tested in our laboratory. Figure 11 compares the measured magnetic flux density in the radial direction along the shell–to–core and pole–face–to–core gaps with the values predicted by finite element analysis, for no current in the coil. The measured peak value is lower, but is spread over a wider axial distance. There is good agreement, especially over most of the shell–to–core gap, where near–zero values of flux density are crucial to achieve force versus position linearity. The actual actuator force is plotted against position for a number of values of coil current in Figure 12. The measured values of force are greater, in each case, than the predicted values since most of the small amount of leakage flux across the shell–to–core gap was neglected in calculating the predicted forces. Moreover, since the coil does see slightly greater total flux as it moves into the actuator, because of the small amounts of leakage, the forces measured increase somewhat with such motion. However, for low values of current and for coil positions that do not place it very near the closed end of the actuator, the actual forces deviate by less than 10% from the predicted values.

5. CONCLUSION

The rig designed to demonstrate vibration isolation to microgravity levels in one–dimension has been built and assembled. Measurements of the background acceleration levels have also been made, and the quietest period for operation has been determined. A compact, long stroke Lorentz actuator has also been designed, built, and tested. Its performance has been shown to match that predicted by finite element analysis very well. Microgravity isolation experiments will be conducted in the very near future.

6. REFERENCES

1. Feuerbacher, B., "Introduction," Chapter 1, Materials Sciences in Space, Ed. B. Feuerbacher, et al., Springer–Verlag, Berlin, 1986.

2. Hamacher, H., "Simulation of Weightlessness," Chapter 3, Materials Sciences in Space, Ed. B. Feuerbacher, et al., Springer–Verlag, Berlin, 1986.

3. Teledyne Brown Engineering, "Low Acceleration Characterization of Space Station Environment," Report No. SP858–MSFC–2928, Oct. 1985.

4. Chase, T.L., "Report on Micro–g Measurements for Space Shuttle Experiments," NASA Lewis Research Center, Dec. 1985.

5. Teledyne Brown Engineering, Abstracts, Workshop on Measurement and Characterization of the Acceleration Environment on Board the Space Station. Guntersville, Alabama, Aug. 11–14, 1986.

6. Hamacher, H., R. Jilg and U. Merbold, "Analysis of Microgravity Measurements Performed During D1," 6th European Symposium on "Materials Sciences under Microgravity Conditions." Bordeaux, Dec. 2–5, 1986.

7. Booz, Allen & Hamilton, "Overview of Space Station Microgravity Requirements," report presented to Dr. J.–D. Bartoe, Chief Scientist, Office of Space Station, July 14, 1989.

8. McDonnell Douglas Corporation "Space Station Definition and Preliminary Design," WP–02, DR–02, Book 22, Section 8 (Loads and Structural Dynamics), Dec. 1985.

9. Ramachandran, N., and C.A. Winter, "The Effects of g–Jitter and Surface Tension Induced Convection on Float Zones," 28th Aerospace Sciences Meeting, AIAA, Reno, Nevada, Jan. 8–11, 1990.

10. Armentrout, R.W., "Two–Body Dynamic simulation of Space Station Exercise Treadmill Including Startup Transient Effects," Memo No. A96–J749–STN–M–RWA–900006, Jan. 10, 1990.

11. Owen, R.G., and D.I. Jones, "Columbus Applications Study (WP. 1.1)," Technical Note No. BTN–001, University College of North Wales, School of Electronic Engineering Science, Bangor, Gwynedd, Sep. 1988.

12. Naumann, R.J. and D.D. Elleman, "Containerless Processing Technology," Chapter 12, Materials Sciences in Space, Ed. B. Feuerbacher, et al., Springer–Verlag, Berlin, 1986.

13. Hendricks, C.D., "Levitation, Coating, and Transport of Particulate Materials," Materials Processing in the Reduced Gravity Environment of Space, Ed. G.E. Rindone, et al., vol. 9, pp. 59, Elsevier Science Publishing Co., Amsterdam, 1982.

14. Rhim, W.–K., M. Collender, M.T. Hyson, W.T. Sims and D.D. Elleman, "Development of Electrostatic Positioner for Space Materials, Processing," Rev. Sci. Instrum., vol. 56, no. 2, p. 307, 1985.

15. Frost, R.T. and C.W. Chang, "Theory and Applications of Electromagnetic Levitation," Materials Processing in the Reduced Gravity Environment of Space, Ed. G.E. Rindone, et al., vol. 9, pp. 71, Elsevier Science Publishing Co., Amsterdam, 1983.

16. Grodsinsky, C.M. and G.V. Brown, "Nonintrusive Inertial Vibration Isolation Technology for Microgravity Space Experiments," submitted for publication to Journal of Spacecraft and Rockets, AIAA, Jan. 1990.

17. Allaire, P.E., M.A. Scott and B.B. Banerjee, "Magnetic Actuators for Microgravity Space Isolation," Workshop on Vibration Isolation Technology for Microgravity Science Experiments," NASA Lewis, Cleveland, Ohip, Sep. 28–29, 1988.

18. Banerjee, B.B., "Analysis and Design of Magnetic Thrust Bearings," M.S. Thesis, Univ. of Virginia, Charlottesville, May 1988.

19. Allaire, P.E., A. Mikula, B.B. Banerjee, D.W. Lewis and J. Imlach, "Design and Test of a Magnetic Thrust Bearing," Journal of the Franklin Institute, vol. 326, no. 6, pp. 831–847, 1989.

20. Allaire, P.E., J. Imlach, J.P. McDonald, R.R. Humphris, D.W. Lewis, B.B. Banerjee, B.J. Blair, J. Claydon and R.D. Flack, "Design, Construction and Test of Magnetic Bearings in an Industrial Canned Motor Pump," Proc. of the Sixth International Pump Users Symposium, Texas A&M Univ., College Station, Nov. 1988.

21. Havenhill, D.D. and K.D. Kral, "Payload Isolation Using Magnetic Suspension," AAS 85–014, Annual AAS Guidance and Control Conference, Keystone, Colorado, Feb. 2–6, 1985.

22. Allen, T.S., D.D. Havenhill and K.D. Kral, "FEAMIS: A Magnetically Suspended Isolation System for Space–Based Materials Processing," AAS 86–017, Annual AAS Guidance and Control Conference, Keystone, Colorado, Feb. 1–5, 1986.

23. Hamilton, B.J., J.H. Andrus and D.R. Carter, "Pointing Mount with Active Vibration Isolation for Large Payloads," AAS 87–033, Annual AAS Guidance and Control Conference, Keystone, Colorado, Jan. 31 – Feb. 4, 1987.

24. Jones, D.I., A.R. Owens, R.G. Owen and G. Roberts, "Microgravity Isolation Mount: Design Report," Technical Note No. BTN–009, University College of North Wales, School of Electronic Engineering Science, Bangor, Gwynedd, Sep. 1989.

25. Sutliff, T., "Vibration Isolation: Airpot (Dashpot) Damping Evaluation," PIR No. 89–9, NASA, Lewis, Cleveland, Ohio, 1989.

26. Hampton, R.D. and C.R. Knospe, "Extended H_2 Synthesis for Multiple–Degree–of–Freedom Controllers," International Symposium on Magnetic Suspension Technology, NASA CP–3152, 1992.

27. Banerjee, B.B., P.E. Allaire and C.R. Knospe, "Vibration Isolation of Science Experiments in Space – Design of a Laboratory Test Setup," Workshop on Aerospace Applications of Magnetic Suspension Technology, NASA CP–10066 Part 2, Paper 26, March 1991.

28. Carlson, A.B., D.G. Gisser and F.K. Manasse, "Magnetics and Electromechanics," Chapter 17, Electrical Engineering: Concepts and Applications, Addison–Wesley Publishing Company, Reading Massachusetts, 1989.

29. McCaig, M. and A.G. Clegg, Permanent Magnets in Theory and Practice, John Wiley & Sons, New York, 1987.

Table 1: Typical Disturbance Environment on a Spacecraft

	QUASI-STEADY ACCELERATIONS	
1e-7 g	(0 to 1e-3) Hz	Aerodynamic Drag
1e-8 g	(0 to 1e-3) Hz	Light Pressure
1e-7 g	(0 to 1e-3) Hz	Gravity Gradient
	PERIODIC ACCELERATIONS	
1e-2 g	9 Hz	Thruster Fire (Orbital)
1e-3 g	(5 to 20) Hz	Crew Motion
1e-4 g	17 Hz	Ku Band Antenna
	NON-PERIODIC ACCELERATIONS	
1e-4 g	1 Hz	Thruster Fire (Attitudinal)
1e-4 g	1 Hz	Crew Push-Off

Table 2: Design Specifications for the Lorentz Actuator

LORENTZ ACTUATOR : FINAL DESIGN	
Total length	= 3.87 in
Magnet outer diameter	= 1.95 in
Magnet inner diameter	= 1.25 in
Magnet length	= 2.77 in
Shell outer diameter	= 1.68 in
Pole-piece thickness	= 0.80 in
Core diameter	= 0.75 in
Air gap	= 0.17 in
Shell-to-core gap	= 0.25 in
Gap ratio	= 1.47 : 1
Coil length	= 4.00 in
Coil wire diameter	= 26.67 mils
Number of turns	= 600 turns
Number of layers	= 4 layers
Maximum coil current	= 2.5 A
Air gap flux density	= 0.145 T
Max. force generated	= 1.25 lbf
Actuator wt. (no coil)	= 2.28 lbf

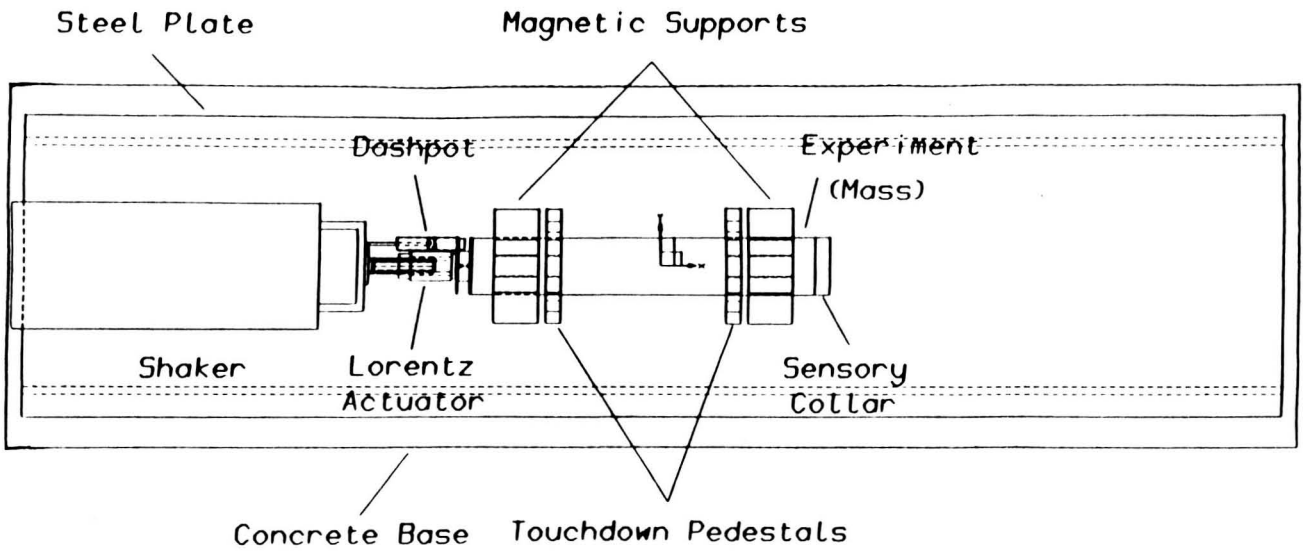

Fig. 1: Design Drawing of the Experiment Rig

ORIGINAL PAGE
BLACK AND WHITE PHOTOGRAPH

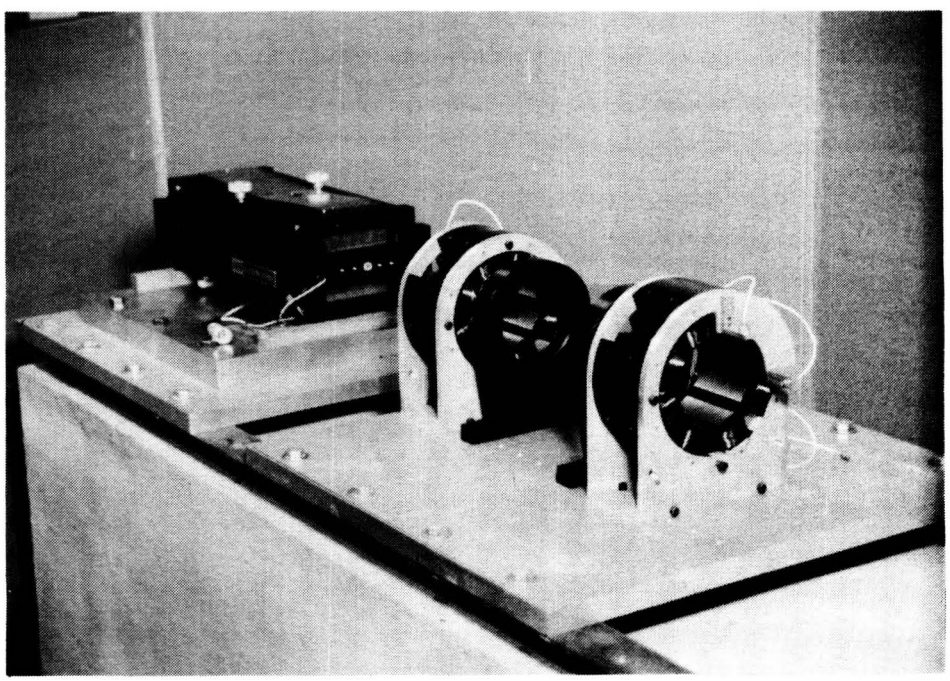

Fig. 2: The Experiment Rig Partially Assembled

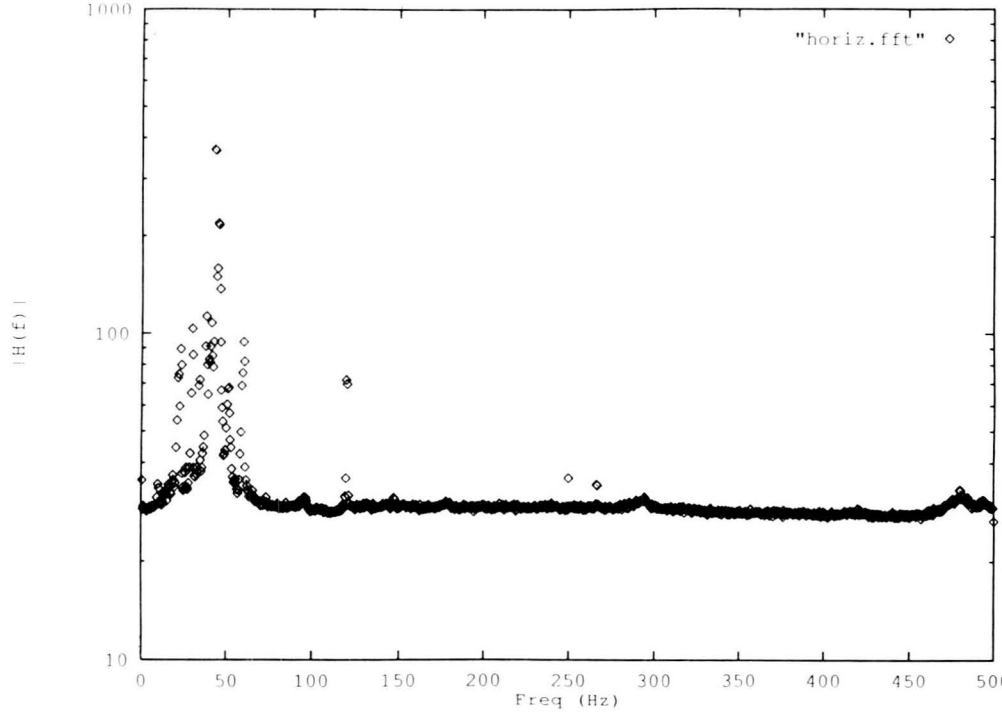

Fig. 3: Background Vibration in the Laboratory -- Horizontal

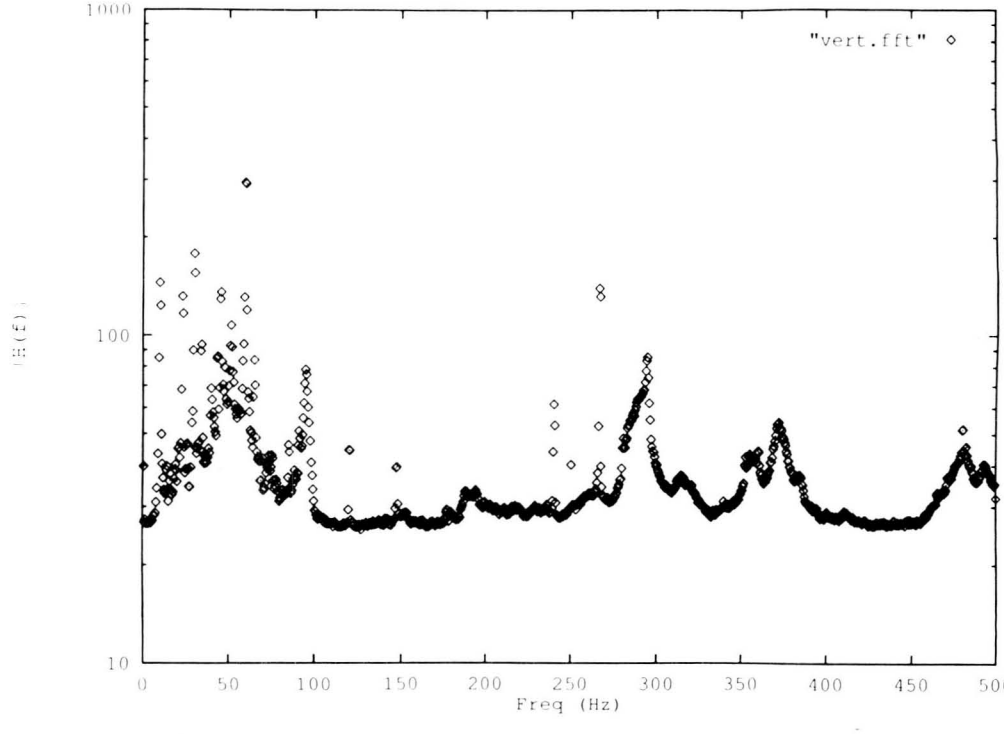

Fig. 4: Background Vibration in the Laboratory -- Vertical

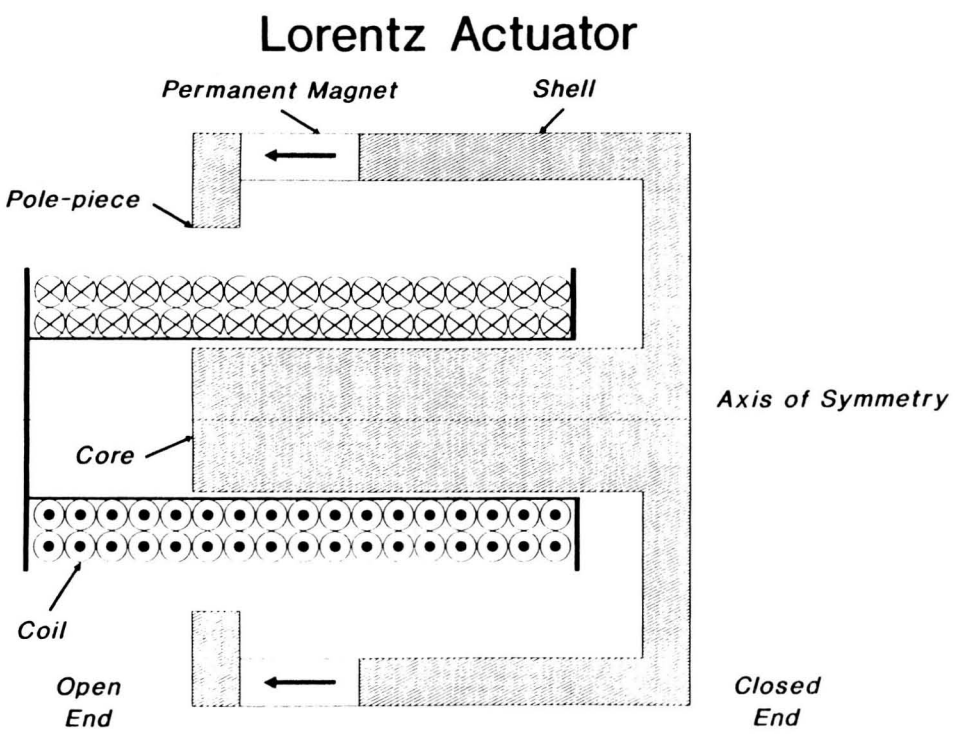

Fig. 5: Schematic of a Lorentz Actuator

LORENTZ ACTUATOR : DESIGN EQUATIONS

1. Assume permanent magnet operating point for maximum energy product : (-H1, B1).
2. Compute magnet flux, fm = B1 • Am.
3. Compute circuit flux, fc = H1 • Lm / R, where R is the circuit reluctance.
4. Compare fm and fc.
5. Adjust operating point until fm = fc = f, the actual operating point. (When saturated, f = saturation flux in saturated segment of circuit.)
6. Calculate air gap flux density, Bg = f / Ag.
7. Compute force capability, F = i • l • Bg, where i is the actuator current and l is the total length of coil wire in the air gap.
8. Change actuator geometry or circuit / magnet material until desired force level is achieved.

Fig. 6: A Simple Algorithm for Designing a Lorentz Actuator

Fig. 7: The Compact, Long-Stroke Lorentz Actuator

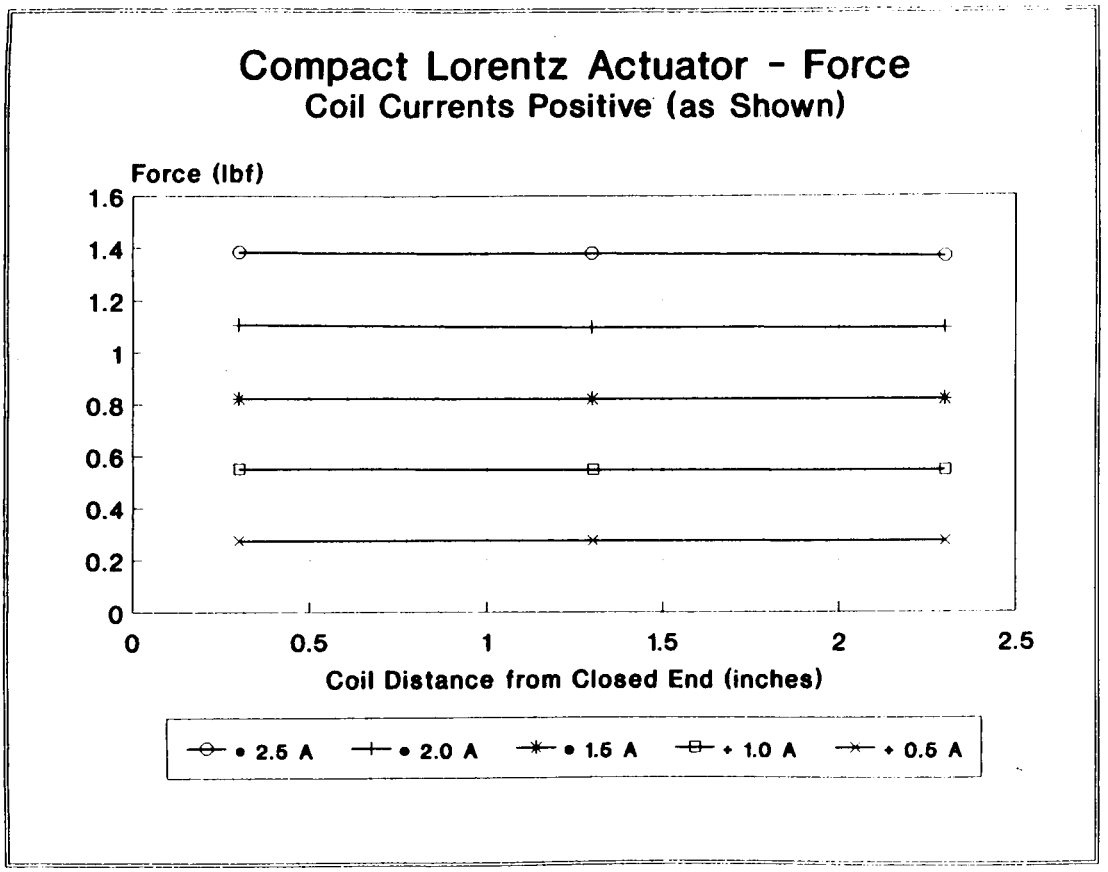

Fig. 8: Force vs. Position (for Positive Coil Currents)

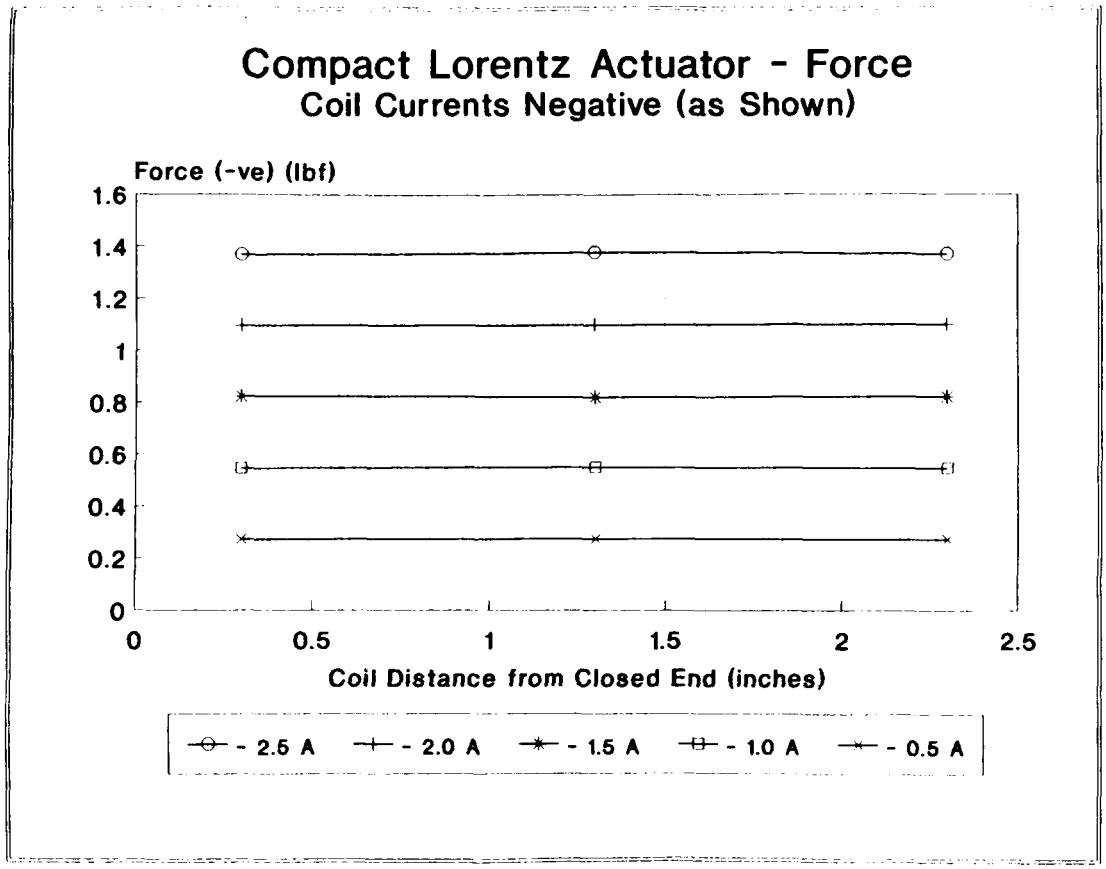

Fig. 9: Force vs. Position (for Negative Coil Currents)

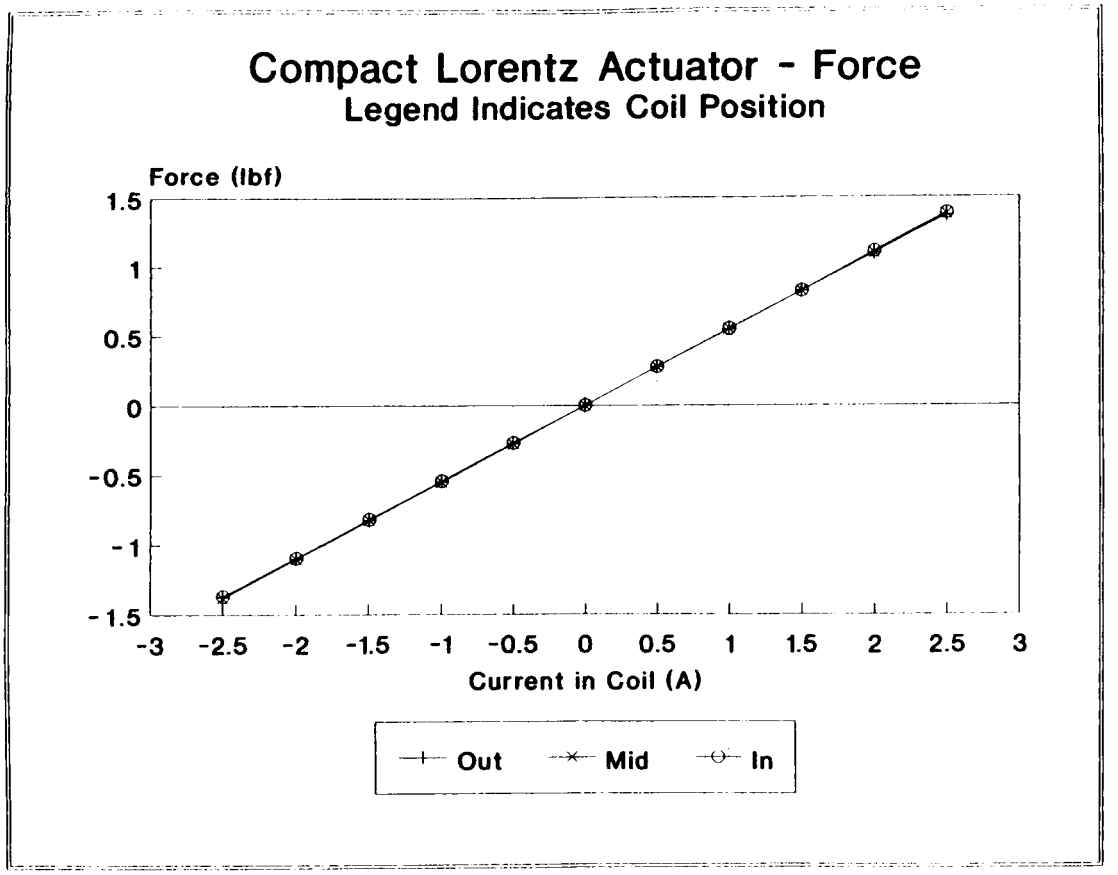

Fig. 10: Force vs. Current (for Three Different Coil Positions)

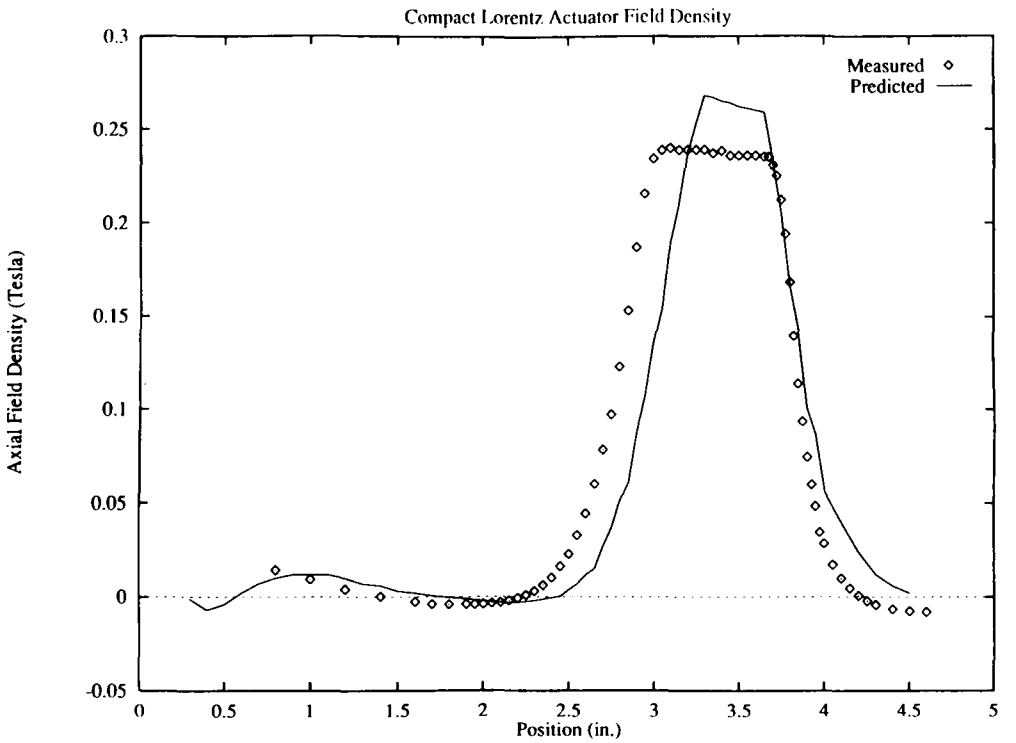

Fig. 11: Comparison of Actual Flux Density with Predicted Values (for No Current in the Coil)

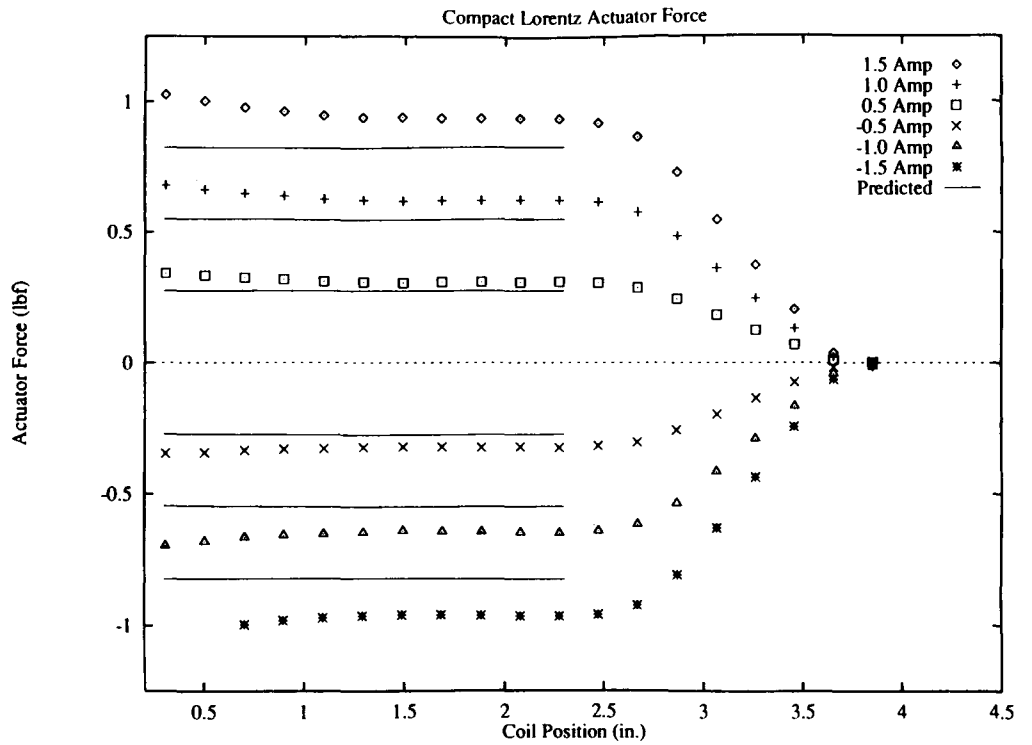

Fig. 12: Comparison of Actual Force vs. Position Characteristics with Analytical Predictions